Please cite this document as: Singh, K., Gardoni, P., & Stochino, F. (2020). Probabilistic models for blast parameters and fragility estimates of steel columns subject to blast loads. *Engineering Structures*, *222*, 110944. DOI: 10.1016/j.engstruct.2020.110944

# Probabilistic models for blast parameters and fragility estimates of steel columns subject to blast loads

Karandeep Singh[1], Paolo Gardoni[2] and Flavio Stochino[3*]

[1] Department of Civil and Environmental Engineering, University of Illinois, 3118 Newmark Civil Engineering Laboratory, 205 N. Mathews Ave. Urbana, IL 61801; Email: ksingh14@illinois.edu

[2] Department of Civil and Environmental Engineering, University of Illinois, 3118 Newmark Civil Engineering Laboratory, 205 N. Mathews Ave. Urbana, IL 61801; Email: gardoni@illinois.edu

[3] Department of Civil Engineering, Environmental and Architecture, University of Cagliari, Building A - Via Marengo 2, 09123 Cagliari (CA) Italy; Email: fstochino@unica.it

*Corresponding Author



## Abstract

This paper proposes a probabilistic framework to predict the failure probabilities of steel columns subject to blast loads. The framework considers the uncertainties in the blast phenomenon, the demands imposed on the column, and the capacities of the column for the limit states of flexure, and global buckling. As part of the work, we propose four probabilistic blast load models. For different types of explosives and atmospheric conditions, two models predict the incident and reflected peak pressure generated by the explosion and two models predict the incident and reflected positive time duration of the blast wave. The models are probabilistic to capture the associated uncertainties, including variations in the atmospheric conditions, the inherent variability in the blast load data even for identical experimental conditions, and model error. The blast load models are used to predict the structural demands (maximum internal moment and deflection) imposed by the blast on a column. The demand models are combined with strain-rate dependent capacity models for flexure and global buckling to estimate the conditional probability of failure

(or fragility) of a steel column for given scaled distance. As an example, fragility estimates for different columns representative of typical columns in steel frames are developed. The results highlight the importance of the explosive weight and column axial load on the failure probabilities.

Keywords: Blast loading; Fragility estimates; Probabilistic blast models; Steel column; SDOF analysis

## 1. Introduction

With rapid industrialization and increasing terrorism threats in the last decade, the need for protecting structures against accidental and intentional blasts has gained significant attention (Hao et al., 2016; Zhang et al., 2019; Draganić et al., 2019). Many buildings that can be exposed to blast loads of varying intensities are steel frame structures (Krauthammer et al, 1990). Therefore, the response of steel frames and their components to blast loads has been widely studied in recent years (e.g.; Sabuwala et al., 2005; Khandelwal et al., 2009; Lee et al., 2009; Urgessa & Arciszewski, 2011; Heidarpour & Bradford, 2011; Nassr et al., 2013; Dragos & Wu, 2014). Some studies focusing on progressive collapse of steel frames due to blast loading have established that the failure of the columns causes the structural collapse (Hamburger & Whittaker, 2004; Krauthammer, 2003). Therefore, adequate design of steel columns is important to ensure the structure's safety against blast loading (Denny et al., 2019; McConnell & Brown, 2011).

Proper design of steel columns against blast loads requires the knowledge of the parameters of the transient, high-pressure wave generated by an explosion. Therefore, the pressure-time variation of a blast wave is of great significance for structural analysis. The pressure-time profile of a blast wave is determined through the peak overpressure, $P_s$ and the positive phase duration, $t_{d,i}$. The blast wave is often reflected by surrounding surfaces which increases the peak overpressure. The increased pressure is referred to as the peak reflected overpressure, $P_r$, with the corresponding positive phase duration defined as $t_{d,r}$. It is generally assumed that $t_{d,i}$ and $t_{d,r}$ have the same value. However, Henrych, (1979) and Shi et al. (2008) reported different values for $t_{d,i}$ and $t_{d,r}$.

Empirical equations are widely used to determine $P_s$, $P_r$, $t_{d,i}$ and $t_{d,r}$ (e.g. Kingery, 1966; Henrych, 1979; Kingery & Coulter, 1983; Ngo et al.; 2007 Karlos et al., 2017). The empirical equations are generally deterministic and do not capture the variability in the blast parameters due to uncertainties in the mass of the explosive, atmospheric conditions, distance of the explosive from the target and inherent variability in the phenomenon (Netherton & Stewart, 2010). Recent studies have aimed at developing probabilistic models for $P_r$ and $t_{d,i}$ (Netherton & Stewart, 2010; Campidelli et al., 2015). Both studies considered the variabilties in the charge mass, atmospheric conditions, and distance between the explosive and the target. In addition, Netherton & Stewart 2010 considered the inherent variability and the difference between deterministic models and experimental data, i.e., the model error, and modeled them as normally distributed variables. The distribution parameters (mean and standard deviation) for the inherent variability were assigned values based on experience and were assumed to be same for both $P_r$ and $t_{d,i}$. However, the choice of normal distribution can give negative values for the parameters that are non-negative in nature. Both studies do not present models for $P_s$, and $t_{d,i}$

The probabilistic collapse analysis of steel frames has been the subject of numerous studies (e.g., Asprone et al., 2008; Asprone et al., 2010; Ding et al., 2017). Ding et al. (2017) considered the effect of the blast load on the member capacity but did not distinguish between the different limit states. Karlos et al. (2017) presented failure curves for steel columns subject to blast loads using the probabilisitc models presented in Netherton & Stewart (2010). In the study global buckling was assumed as the predominant failure mode. However, the work does not consider the inherent variability and the effect of atmospheric conditions, charge mass and other factors affecting the blast parameters.

This paper develops probabilistic models for incident and reflected blast parameters $P_s$, $P_r$, $t_{d,i}$ and $t_{d,r}$. The proposed models are developed by combining information from existing empirical equations with information available from blast tests presented in Hoffman & Mills (1956). A Bayesian approach is used to estimate unknown model parameters. The Bayesian approach makes it possible to efficiently update the model parameters when new data becomes available. The proposed models identify the parameters that significantly affect the characteristics of blast waves. The developed models are then used to predict the structural demands (maximum internal moment and deflection) imposed by the blast on a column. The paper uses a pinned-hinged steel column presented in Nassr (2012) to predict the response. The demand models are combined with strain-dependent capacity models for flexure and global buckling to estimate the conditional probability of failure (or fragility) of a steel column for given scaled distance. As an example, fragility curves for a typical column are developed. The results highlight the effects of the charge weight and the axial load on the failure probabilities. The results provide valuable information that can be used to develop efficient blast-resistant designs of steel frame buildings for different scenarios. The paper also presents fragility curves for the serviceability limit state of flexure which can be used within a life-cycle analysis framework (Jia, et al., 2017).

Following this introduction, the next section discusses the experimental data used for developing the models. Next, we present the proposed models and discuss the general formulation. The next section discusses the capacity and demand models chosen for the considered limit states. Finally, the paper presents the assessment of the structural fragility of steel columns and compares the effects of the charge weight and the axial load.

## 2. Data for constructing probabilistic blast parameter models

For developing the proposed probabilistic models, we use data from experimental blast load tests available in Hoffman & Mills (1956). Along with the observation for blast parameters, the database contains information about ambient pressure ($P_a$), ambient temperature ($T_a$), charge weight ($W$), and scaled distance ($Z$) for each test. The scaled distance is commonly used to determine pressure-time profile of a blast wave and is defined as

$$Z = R / W^{1/3} \tag{1}$$

where $R$ is the distance of the explosive from the point of interest. In this paper, we also introduce the radius of explosive, $r$, as a dependent variable. For the sake of simplicity, we define the dependent variables as vector $\mathbf{x}$, i.e., $\mathbf{x} = \{Z, W, P_a, T_a, r\}$

For some blast parameters, there were multiple gauges to record the data. However, the observed values of the parameters for some of the tests were not recorded or were illegible in the best available reproduction of the reference document. The usable data are available for 185, 191, 158 and 186 tests for $P_s$, $P_r$, $t_{d,i}$ and $t_{d,r}$, respectively. Table 1 gives the range for relevant parameters, where $r$ is the explosive's radius, calculated using pentolite density of $\rho = 1650$ kg/m$^3$.

Please cite this document as: Singh, K., Gardoni, P., & Stochino, F. (2020). Probabilistic models for blast parameters and fragility estimates of steel columns subject to blast loads. *Engineering Structures*, *222*, 110944. DOI: 10.1016/j.engstruct.2020.110944

**Table 1: Range of the values of the blast parameters and the physical regressors in the experimental data**

| Blast Parameter | Symbol | Range |
|---|---|---|
| Incident Peak Pressure (MPa) | $P_s$ | 0.025-3.586 |
| Reflected Peak Pressure (MPa) | $P_r$ | 0.056-25.420 |
| Incident Positive Phase Duration (sec) | $t_{d,i}$ | 0.116-3.375 |
| Reflected Positive Phase Duration (sec) | $t_{d,r}$ | 0.167-3.439 |
| Dependent variables | | |
| Scaled distance ($\mathrm{m/kg^{1/3}}$) | $Z$ | $0.59-5.87$ |
| `Explosive weight (kg) | $W$ | $0.24-4.1$ |
| Ambient pressure (hPa) | $P_a$ | $1005-1032$ |
| Ambient temperature ($^\circ\mathrm{C}$) | $T_a$ | $3.3-33.2$ |
| Explosive radius (m) | $r$ | $0.03-0.085$ |

## 3. Formulation of probabilistic blast parameter models

To assess the fragility of a steel column subject to a blast load, we need to estimate the blast parameters $P_s$, $P_r$, $t_{d,i}$ and $t_{d,r}$. Gardoni et al. 2002 and Gardoni et al. 2003, proposed a general model form to develop unbiased probabilistic models that capture our understanding of the underlying physics of a phenomenon and at the same time capture data available from laboratory testing and/or field measurements. In this section, we develop probabilistic models for the blast parameters based on Gardoni et al.'s formulation. To promote the practical use of the developed models, the models start from accepted deterministic models. Correction terms are then added to the model to remove the possible bias in the current models and improve the quality of the model, and a model error term is also added to the model to capture the remaining variability that may arise due to inaccurate model form, missing variables, and statistical uncertainties. The general model form can be written as

$$A_k\left(\mathbf{x},\mathbf{\Theta}_k\right)=\hat{A}_k\left(\mathbf{x}\right)+\gamma_k\left(\mathbf{x},\mathbf{\theta}_k\right)+\sigma_k\varepsilon_k \tag{2}$$

where $A_k(\mathbf{x},\mathbf{\Theta}_k)$ is either the blast parameter of interest or a transformation of the parameter of interest; the index $k$ denotes the specific parameter of interest, (i.e. $k=1,2,3,4$ represent $P_s$, $P_r$, $t_{d,i}$ and $t_{d,r}$); $\mathbf{x}$ represents the measurable variables including environmental variables, material and geometric properties affecting the blast parameters; $\mathbf{\Theta}_k=(\mathbf{\theta}_k,\sigma_k)$ is a vector of unknown parameters to be estimated; $\hat{A}_k(\mathbf{x})$ is an existing deterministic model for the parameter of interest or it's transformation; $\gamma_k(\mathbf{x},\mathbf{\theta}_k)$ is the correction term; and $\sigma_k\varepsilon_k$ is the model error which is assumed to be additive (additivity assumption), where $\sigma_k$ is the standard deviation of the model error independent of $\mathbf{x}$ (homoskedasticity assumption) and $\varepsilon_k$ is standard normal variable (normality assumption). To satisfy the additivity, homoskedasticity and normality, we can use an appropriate variance stabilizing transformation, such as those mentioned in Box & Cox, 1982**.** In this paper, we use a logarithmic transformation of the blast parameters to define $A_k(\mathbf{x},\mathbf{\Theta}_k)$ and of the deterministic model to define $\hat{A}_k(\mathbf{x})$.

Following Gardoni et al. (2002), we use a functional form, linear in $\mathbf{\theta}_k$, for $\gamma_k(\mathbf{x},\mathbf{\theta}_k)$, which is defined as follows:

$$\gamma_k(\mathbf{x}, \boldsymbol{\theta}_k) = \sum_{i=1}^{p} \theta_{k,i} h_{k,i}(\mathbf{x}) \tag{3}$$

where $h_{k,i}(\mathbf{x})$'s are explanatory functions obtained from appropriate box-cox transformation of basis functions of $\mathbf{x}$, $\eta_{k,i}(\mathbf{x})$ (i.e., $h_{k,i} = \eta_{k,i}^{\lambda_{k,i}}(\mathbf{x})$ where $\boldsymbol{\Lambda}_k = (\lambda_{k,1}, \dots, \lambda_{k,p})$ is a vector of unknown exponents), and $\theta_{k,i}$ are the components of the vector $\boldsymbol{\theta}_k$.

*3.1. Box-cox transformation, Bayesian updating and model selection*

We can estimate $\boldsymbol{\Lambda}_k$ and $\boldsymbol{\Theta}_k$ simultaneously using nonlinear regression or estimate $\boldsymbol{\Lambda}_k$ followed by $\boldsymbol{\Theta}_k$, as detailed in Tabandeh & Gardoni (2014). However, the authors noted that the former method involves high computational time and may give inaccurate results with increasing number of regressors. Hence, we will estimate $\boldsymbol{\Lambda}_k$ followed by $\boldsymbol{\Theta}_k$, which was found to give estimates comparable to those obtained using nonlinear regression.

Following Tabandeh & Gardoni (2014), we use maximum likelihood criterion to estimate $\boldsymbol{\Lambda}_k$ and the log-likelihood function takes the form:

$$\ln\left[L_k\left(\boldsymbol{\Lambda}_k\right)\right] \propto -\frac{n}{2}\ln\left(2\pi\right) - \frac{n}{2}\ln\left(|\,\hat{\mathbf{V}}_k(\boldsymbol{\Lambda}_k)\,|\right) - \frac{n}{2} \tag{4}$$

where $\hat{\mathbf{V}}_k(\boldsymbol{\Lambda}_k)$ is the covariance matrix of the random functions $\mathbf{h}_k(\mathbf{x}_q) = [\eta_{k,1}^{\lambda_{k,1}}(\mathbf{x}_q), \dots, \eta_{k,p}^{\lambda_{k,p}}(\mathbf{x}_q)]^T$ and $q = 1, \dots, n$ is the index for the $q^{th}$ observation in a sample set of $n$ observations.

From Eq. (4), we can observe that the minimum of the determinant of $\hat{\mathbf{V}}_k(\boldsymbol{\Lambda}_k)$ corresponds to the estimates for $\boldsymbol{\Lambda}_k$. Following Weisberg 2005, $\hat{\mathbf{V}}_k(\boldsymbol{\Lambda}_k)$ takes the form:

$$\hat{\mathbf{V}}_k(\mathbf{\Lambda}_k)=\frac{1}{n}\sum_{q=1}^{n}\left\{\left[\mathbf{h}_k\left(\mathbf{x}_q\right)-\frac{1}{n}\sum_{q=1}^{n}\mathbf{h}_k\left(\mathbf{x}_q\right)\right]\left[\mathbf{h}_k\left(\mathbf{x}_q\right)-\frac{1}{n}\sum_{q=1}^{n}\mathbf{h}_k\left(\mathbf{x}_q\right)\right]^T\right\} \tag{5}$$

After obtaining $h_i(\mathbf{x})$'s using box-cos transformation, we estimate $\mathbf{\Theta}_k$ using the Bayesian updating rule, defined as:

$$f\left(\mathbf{\Theta}_k\right)=\xi_k L\left(\mathbf{\Theta}_k\right)p\left(\mathbf{\Theta}_k\right) \tag{6}$$

where $f(\mathbf{\Theta}_k)$ is the posterior distribution reflecting the updated state of information about $\mathbf{\Theta}_k$; $L(\mathbf{\Theta}_k)$ is the likelihood function capturing the information from the data; $p(\mathbf{\Theta}_k)$ is the prior information which reflects the available information before collecting the data; and $\xi_k=[\int L(\mathbf{\Theta}_k)p(\mathbf{\Theta}_k)d\mathbf{\Theta}_k]^{-1}$ is a normalizing factor. For multidimensional problems where $L(\mathbf{\Theta}_k)p(\mathbf{\Theta}_k)$ is not proportional to a familiar probability distribution function, predicting $\xi_k$ can be challenging. In this paper, we use the Delayed Rejection Adaptive Metropolis DRAM method (Haario et al., 2006), an adaptive delayed rejection Markov Chain Monte Carlo MCMC simulation method to estimate the posterior statistics of the unknown model parameters.

The experimental data of blast parameters often contains observations which include measurement errors because of gauge malfunction, gauge hysteresis and base line drift (Kingery, 1966). Moreover, the variables in $\mathbf{x}$ may have associated variabilities which are not reflected in the database. Therefore, $L(\mathbf{\Theta}_k)$ needs to be written in a way to reflect the measurement errors associated with the parameters of interest and dependent variables. Assuming statistical independence between different observations and absence of systematic error in the measurements, $L(\mathbf{\Theta}_k)$ can be written, as per Gardoni et al. (2002) and Tabandeh & Gardoni (2014), as:

$$\ln\left(L(\boldsymbol{\Theta}_k)\right) \propto \sum_{\text{failure data}} \left\{ \frac{1}{\hat{\sigma}_k\left(\boldsymbol{\theta}_k, \sigma_k\right)} \varphi\left[ \frac{\hat{r}_{k,i}\left(\boldsymbol{\theta}_k\right)}{\hat{\sigma}\left(\boldsymbol{\theta}_k, \sigma_k\right)} \right] \right\} \tag{7}$$

where $\hat{r}_{k,i}(\boldsymbol{\theta}_k) = \hat{A}_{k,i} - \hat{A}(\hat{\mathbf{x}}_i) - \gamma(\hat{\mathbf{x}}_i, \boldsymbol{\theta}_k)$ is the prediction residual for $i^{th}$ observation with $\hat{A}_i$ and $\hat{\mathbf{x}}_i$ being the measured observation and variable values; $\hat{\sigma}_k(\boldsymbol{\theta}_k, \sigma_k) = \sqrt{\sigma_k^{\ 2} + s_k^2 + \nabla_{\hat{\mathbf{x}},i}\hat{r}_{k,i}(\boldsymbol{\theta}_k)\Sigma\hat{r}_{k,i}(\boldsymbol{\theta}_k)^T}$ is the standard deviation , with $s^2$ and $\Sigma$ as the variance and covariance matrix of measurement errors in $\hat{A}_i$ and $\hat{\mathbf{x}}_i$; and $\nabla_{\hat{\mathbf{x}}_i}$ is the gradient row vector with respect to $\mathbf{x}$. In the absence of any prior information about the model parameters, we use a noninformative prior distribution $p(\boldsymbol{\Theta}_k) \propto 1/\sigma_k$.

To ensure precision in the estimates, obtain small values of $\sigma_k$ and prevent over-fitting of data, $\gamma(\mathbf{x}, \boldsymbol{\theta}_k)$ needs to be parsimonious. The parsimonious form can be obtained using a stepwise deletion process. Following Gardoni et al. (2002), we start with a model including all the explanatory functions and interaction terms and successively eliminate the function with the highest posterior coefficient of variation (COV). In the presence of interaction and higher-order terms, a main effect is removed only after the removal of the associated interaction and higher order terms. The remaining explanatory functions are re-fitted to the data and the process is repeated until every element in $\boldsymbol{\theta}_k$ has COV lower than $\sigma_k$ or there is an unacceptable increase in $\sigma_k$. The definition of an unacceptable increase in $\sigma_k$ is subjective and depends on the desired model accuracy, desired parsimony in the model and the desired variability in the model parameters of $\boldsymbol{\theta}_k$. In the event of strong correlation between two parameters, $\theta_{k,i}$ and $\theta_{k,j}$ (for the

Please cite this document as: Singh, K., Gardoni, P., & Stochino, F. (2020). Probabilistic models for blast parameters and fragility estimates of steel columns subject to blast loads. *Engineering Structures*, *222*, 110944. DOI: 10.1016/j.engstruct.2020.110944

purpose of the paper, we assume a strong correlation when $\left|\rho_{\theta_{k,i}\theta_{k,j}}\right| \geq 0.7$), we can linearly combine them as follows:

$$\hat{\theta}_{k,i} = \mu_{\theta_{k,i}} + \rho_{\theta_{k,i}\theta_{k,j}} \frac{\sigma_{\theta_{k,i}}}{\sigma_{\theta_{k,j}}} \left(\theta_{k,j} - \mu_{\theta_{k,j}}\right) \tag{8}$$

where, $\mu_{\theta_{k,i}}$ and $\sigma_{\theta_{k,i}}$ are the posterior mean and standard deviation of $\theta_{k,i}$, respectively.

*3.2. Model development for peak overpressure and positive time duration*

3.2.1. Deterministic models

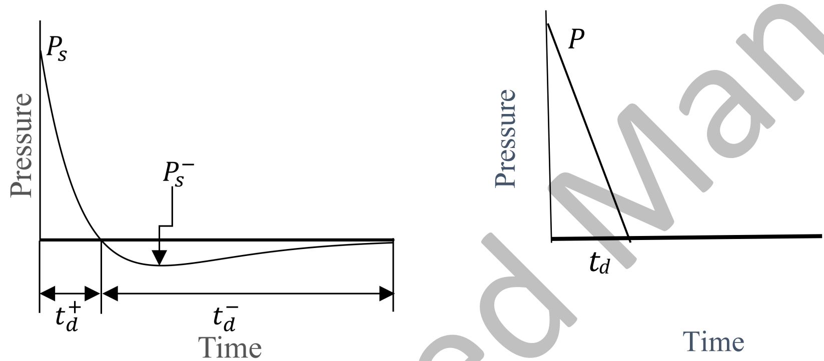


**Fig 1: Pressure – Time profile of a blast wave (left) and linear approximation (right).**

The probabilistic models developed in the paper build upon the deterministic models for the parameters of a blast wave. An explosion causes the formation of a blast wave which decays with time.

An exponential law is typically adopted to describe the time ($t$) history of the blast overpressure, but a good approximation of this behavior can be expressed by a linear function, Karlos & Solomos 2013, Nassr et al. (2012), Nassr et al. (2013), see Figure 1 and Eq. (9).

$$P(t) = P_s\left(1 - \frac{t}{t_d}\right) \tag{9}$$

where $P_s$ is the peak incident overpressure that can be substituted by $P_r$ in case of reflected overpressure, $t_d$ is the positive phase duration. At the time when the blast wave reaches the point of interest, typically called the arrival time $t_a$, the imposed pressure increases instantaneously to a peak overpressure value, $P_s$, over the ambient pressure $P_o$. With time, the pressure decreases and at time $t_{d,i}$, it reaches the ambient pressure. After $t_{d,i}$, the pressure decays further to an under pressure $P_s^-$ and eventually reaches the ambient pressure at time $t_{d,i} + t_{d,i}^-$. Here, $t_{d,i}$ and $t_{d,i}^-$ are the positive phase duration and the negative phase duration of the blast wave respectively. From a structural safety viewpoint, the positive wave duration dominates the structural response. Therefore, this paper only considers the modelling of positive phase duration. With reference with equation (2) the following notation is assumed: $\hat{A}_1 = \hat{P}_R$, $\hat{A}_2 = \hat{P}_s$, $\hat{A}_3 = t_{d,i}$, $\hat{A}_4 = t_{d,r}$.

The parameters of a blast wave are dependent on the shape of the explosive. In this work, we consider only hemispherical explosions. Out of the many empirical relations available in literature, the equations presented in UFC 3-340-02 (2008) are most widely used to estimate the incident and reflected blast parameters for hemispherical explosives. However, the equations for $P_s$ and $P_r$ significantly deviate from the experimental values for $Z \leq 1\ \text{m/kg}^{1/3}$. Therefore, we use the modified equations presented in Karlos & Solomos (2013). corrected for the mentioned discrepancies in $\hat{P}_s$ and $\hat{P}_r$. The following form is adopted to describe the overpressure values:

$$Y = 10^{\sum_{i=o}^{n} c_i U^i} \qquad \text{where} \qquad U = K_0 + K_1 Log(Z) \tag{10}$$

Where Y can represent $\hat{P}_R$ or $\hat{P}_S$ and $C_i$, $K_0$, $K_1$ are constant coefficients determined through a least squares fitting of experimental values. For the sake of clearness one set of coefficients is calculated for $\hat{P}_R$ and one set is calculated for $\hat{P}_S$, see Karlos & Solomos (2013), Karlos et al. (2017) and Kingery C. N., & Bulmash G., (1984).

Following Kinney and Graham (1983), we define the deterministic model for $t_{d,i}$ here denoted as $\hat{A}_3$:

$$\hat{A}_3 = \frac{980\left[1+\left(\frac{Z}{0.54}\right)^{10}\right]}{\left[1+\left(\frac{Z}{0.02}\right)^{3}\right]\left[1+\left(\frac{Z}{0.74}\right)^{6}\right]\sqrt{1+\left(\frac{Z}{6.9}\right)^{2}}} W^{1/3} \quad (11)$$

Shi (2008) and Henrych (1979) observed significant difference between $t_{d,i}$ and $t_{d,r}$ for $Z \le 3$ m/kg$^{1/3}$. Therefore, we use the following equation proposed in Henrych (1979) for $\hat{A}_4$ representing $t_{d,r}$:

$$\hat{A}_4 = \left(0.107 + 0.444Z + 0.264Z^2 - 0.129Z^3 + 0.0335Z^4\right) W^{1/3} \quad (12)$$

The above equation is valid for $Z \le 2.8$ m/kg$^{1/3}$. For $Z > 2.8$ m/kg$^{1/3}$, we use the equation for $t_{d,i}$ presented in UFC 3-340-02 (2008)

3.2.2. Model correction

As initial explanatory functions for all the blast parameters, we select $\eta_{k,1} = 1$ to capture potential model bias, $\eta_{k,2}(\mathbf{x}) = P_a / 1013.25$, $\eta_{k,3}(\mathbf{x}) = 288/(273 + T_a)$, $\eta_{k,4}(\mathbf{x}) = R/r$ and $\eta_{k,5}(\mathbf{x}) = W/\bar{W}$, where 1013.25 is the standard atmospheric pressure in hPa, $\bar{W}$ is the mean weight of the explosives in the tests. We obtain the explanatory functions $h_{k,i}(\mathbf{x})$'s using the methodology explained earlier in the paper and determine that log transformation is suitable for all the candidate functions.

Initially, a linear term of the form $h_k(\mathbf{x}) = \sum_{i=2}^{5} h_{k,i}(\mathbf{x})$. However, the diagnostic plots showed a higher-order relationship with the explanatory functions. Therefore, we propose higher order correction terms with one-way interactions for the initial run. The correction term for the initial run is defined as:

$$h_k(\mathbf{x}) = \sum_{i=2}^{5} h_{k,i}(\mathbf{x}) + \sum_{i=2}^{5} h_{k,i}^2(\mathbf{x}) + \sum_{i=2}^{4} \sum_{j=i+1}^{5} h_{k,i}(\mathbf{x}) h_{k,j}(\mathbf{x}) \tag{13}$$

3.2.3. Measurement errors in the parameters

Blast waves imposes high demands on the instrumentation systems. Therefore, there are many contributors to measurement errors in the observed parameters, including but not limited to, hysteresis, non-linearity, resonances ( Netherton & Stewart, 2010). We define the true value for a parameter of interest as:

$$A_{k,true} = A_{k,inst} A_{k,obs} \tag{14}$$

where $A_{k,obs}$ is the observed value, $A_{k,true}$ is the actual value of the parameter, and $A_{k,inst}$ is the multiplicative measurement error.

The measurement errors depend on the type of recording instrument used. However, there is not enough data available in Hoffman and Mills (1956) to specify the associated instrument error. Netherton (2012) provided a detailed literature review of the instrument tolerances observed in many studies, which can range from $\pm 10\%$ to $\pm 20\%$ for the instrument used in the available data. However, the range of instrument error is narrower than $\pm 10\%$ for the observed values of peak overpressure (Kingery, 1966). Therefore, we propose the measurement errors based on 95% confidence that the tolerance range is $\pm 15\%$ for $t_{d,i}$ and $t_{d,r}$ and $\pm 5\%$ for $P_s$ and $P_r$.

Generally, instrument errors are modeled assuming a normal distribution. However, we can obtain negative values for $A_{k,true}$ if $A_{k,inst}$ is normally distributed. Therefore, we assume a lognormal distribution for $A_{k,inst}$. Taking the mean of $A_{k,inst}$, $\mu_{A_{k,inst}}$, as 1 and assuming 95% confidence interval, we can determine the standard deviation for the measurement error using the following formulation presented in Olsson (2005)

$$\left[ m_{A_{k,inst}} \pm 0.15 m_{A_{k,inst}} \right] = \left[ m_{A_{k,inst}} + \frac{s_{A_{k,inst}}^{\;2}}{2} \pm 2.02 \sqrt{\frac{s_{A_{k,inst}}^{\;2}}{n} + \frac{s_{A_{k,inst}}^{\;4}}{2(n-1)}} \right] \tag{15}$$

where $\mu_{A_{k,inst}}$ and $\sigma_{A_{k,inst}}$ are the mean and standard deviation of $A_{k,inst}$, $m_{A_{k,inst}}$ and $s_{A_{k,inst}}$ are the mean and standard deviation of underlying normal distribution $\ln(A_{k,inst})$ and $n$ is the sample size. Solving the non-linear system of equations, we can find values for $m_{A_{k,inst}}$ and $s_{A_{k,inst}}$, which can be used to calculate $\mu_{A_{k,inst}}, \sigma_{A_{k,inst}}$ using the following equations:

Please cite this document as: Singh, K., Gardoni, P., & Stochino, F. (2020). Probabilistic models for blast parameters and fragility estimates of steel columns subject to blast loads. *Engineering Structures*, *222*, 110944. DOI: 10.1016/j.engstruct.2020.110944

$$\mu_{A_{k,inst}} = \exp\left( m_{A_{k,inst}} + \frac{{s_{A_{k,inst}}}^2}{2} \right) \quad (16)$$
$$\sigma_{A_{k,inst}}{}^2 = \exp\left(2m_{A_{k,inst}} + s_{A_{k,inst}}{}^2\right)\left[\exp\left(s_{A_{k,inst}}{}^2\right) - 1\right]$$

Substituting the system of equations from (14) to (13), we get $\sigma_{A_{k,inst}} = 0.075$ for $t_{d,i}$ and $t_{d,r}$, and $\sigma_{A_{k,inst}} = 0.025$ for $P_s$ and $P_r$.

3.2.4. Variability in charge weight

The charge weight varies due to two factors: (1) user factor $W_{user}$ and (2) Net Equivalent Quantity (NEQ) factor ($W_{NEQ}$), defined as ratio of the energy output of 1 kg of the explosive to the energy output of 1 kg of TNT. $W_{user}$ captures the difference in the charge weight from the desired value due to human error in mass selected. $W_{NEQ}$ signifies the variability in the energy output of a weight of the explosive with respect to an equal weight of TNT. The variation in $W_{NEQ}$ is caused by variations in the explosive's volume and density during manufacture, variations in the explosive's mix during manufacture and other factors associated with use and storage (Netherton, 2012).

Therefore, the total equivalent mass of the explosive $(W)$, in terms of TNT is

$$W = W_d \times W_{user} \times W_{NEQ} \quad (17)$$

where $W_d$ = desired explosive mass, $W_{user}$ = user factor and $W_{NEQ}$ = NEQ factor.

The explosive used in the experiments conducted by Hoffman & Mills (1956) was pentolite. Commercially manufactured explosives like pentolite exhibit very low variability with typical tolerance values lying between $\pm 0.1\% - \pm 0.2\%$ (Kingery, 1966; Netherton, 2012).

Herein, we model $W_{user}$ as a lognormal distribution with a 95% confidence that the tolerance is $\pm 0.1\%$. With the mean of $W_{user}$, $\mu_{W_{user}}$ as 1, we determine the standard deviation, $\sigma_{W_{user}} = 0.0005$ using similar methodology used for determining $\sigma_{A_{k,inst}}$ in Section 3.2.3.

The energy output of Pentolite is higher than that of TNT, for the same explosive mass. However, $W_{NEQ}$ for pentolite exhibits significant variability. Campidelli et al. (2015) analyzed data available for $W_{NEQ}$ of pentolite and determined the mean, $\mu_{W_{NEQ}}$, and standard deviation, $\sigma_{W_{NEQ}}$, as 1.20 and 0.18 respectively. But they assumed $W_{NEQ}$ to be normally distributed, which can generate negative values of $W$. Therefore, we assume a lognormal distribution for $W_{NEQ}$. The mean and standard deviation of the underlying normal distribution, $m_{W_{NEQ}}$ and $s_{W_{NEQ}}$, are 0.1712 and 0.1492, respectively, calculated using Eq. (16). As Eq (7) assumes that the errors are not systematic, we linearly transform the lognormal distribution using the following equation:

$$W_{NEQ} = 1.2\left(\frac{W_{NEQ}}{1.2}\right) = 1.2LN\left[0.1712 + \ln\left(\frac{1}{1.2}\right), 0.149\right] \approx 1.2LN(0, 0.149) = 1.2W'_{NEQ} \tag{18}$$

Using Eq. (17), we obtain $\mu'_{W_{NEQ}} = 1$ and $\sigma'_{W_{NEQ}} = 0.151$. Therefore, the total mass variability $W_{\text{var}} = W_{NEQ} \times W_{user}$ is lognormally distributed with $m_{W_{\text{var}}} = 0$ and $s_{W_{\text{var}}} = 0.151$. The logarithmic transformation of $h_5$ makes the mass variability normally distributed, as required in development of the log-likelihood function. Therefore, we use $m_{W_{\text{var}}}$ and $s_{W_{\text{var}}}$ for developing the log-likelihood function as per Eq. (7).

Please cite this document as: Singh, K., Gardoni, P., & Stochino, F. (2020). Probabilistic models for blast parameters and fragility estimates of steel columns subject to blast loads. *Engineering Structures*, *222*, 110944. DOI: 10.1016/j.engstruct.2020.110944

3.2.5. Parameter estimation and model selection

As there is no prior information available about $\mathbf{\Theta}_k$ for all the blast parameters, we consider a noninformative prior distribution in Eq. (6). In this section, we present the results of stepwise deletion method used to develop parsimonious models for $P_s$, $P_r$, $t_{d,i}$ and $t_{d,r}$.

Fig. 2 shows the posterior COV of $\theta_{1,i}$'s (as dots) and mean of $\sigma_1$ (as an open square) at each step of the deletion process. The deletion process is stopped at the 13th step. Upon examining the correlation coefficients, we observe a high dependence between $\theta_{1,1}$ and $\theta_{1,4}$; and $\theta_{1,1}$ and $\theta_{1,8}$. Given that $h_{1,8}$ is the square of $h_{1,4}$, the high dependence is expected. Using Eq. (8), we combine them and the correction term for $P_s$, $\gamma_1$ is determined to be:

$$\gamma_1\left(\mathbf{x},\mathbf{\Theta_1}\right)=\theta_{1,1}+\left(-0.459-0.905\theta_{1,1}\right)\left[\ln\left(\frac{R}{r}\right)\right]+\left(1.55+0.947\theta_{1,1}\right)\left[\ln\left(\frac{R}{r}\right)\right]^2 \tag{19}$$

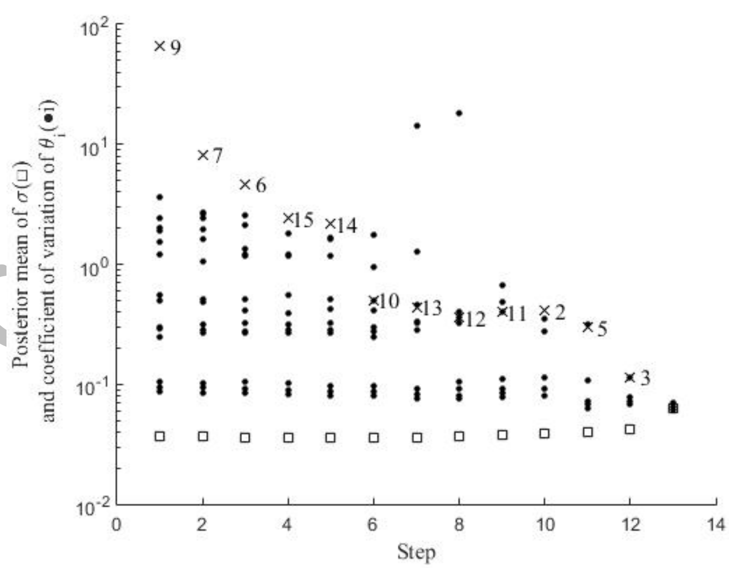


**Fig 2: Stepwise deletion for $\mathbf{\Theta}_1$, the cross points at the parameter with the higher coefficient of variation for each step.**

Table 2 lists the posterior statistics of $\mathbf{\Theta}_1$. The correction term $h_{1,4}$ is a non-dimensional representation of the information contained in $Z$. Therefore, the used deterministic equation of $P_s$, which is a function of $Z$, does not completely represent the contribution of scaled distance.

**Table 2: Posterior statistics of $\mathbf{\Theta}_1$**

| Parameter | Mean | St. Dev. | Correlation Coefficients | |
|---|---|---|---|---|
| | | | $\theta_{1,1}$ | $\sigma_1$ |
| $\theta_{1,1}$ | −1.80 | 0.124 | 1 | |
| $\sigma_1$ | 0.053 | 0.004 | −0.058 | 1 |

Fig 3 shows a comparison between the measured and predicted values of $P_s$ based on the deterministic (left) and probabilistic (right) models. A visual inspection of the deterministic plot shows that the deterministic model underestimates the value. Therefore, the intercept was expected to be positive. However, the mean value for the intercept is negative. The negative term of the intercept is present because the present square term underfits the data for high values of $P_s$. The plot for probabilistic model includes two 15% and 85% bounds for the data, the true model error (in dashed lines); and including the standard deviation of the measurement error (in dash-dot lines). It can be observed that the correction terms effectively correct the bias in the deterministic model. It can be observed that the model does not affect the variability in the observed values for repeat observations. The variability can be attributed to the measurement error in the variables, and missing variables. The effect of the measurement error can be checked by plotting the median

Please cite this document as: Singh, K., Gardoni, P., & Stochino, F. (2020). Probabilistic models for blast parameters and fragility estimates of steel columns subject to blast loads. *Engineering Structures*, *222*, 110944. DOI: 10.1016/j.engstruct.2020.110944

values of the ratio of observed and predicted values for repeat observations. The median values are represented by the crosses in the figure. For the probabilistic model, most of the median values lie evenly between the one standard deviation limits of the true model error. Also, most of the data points lie between the combined bounds. Therefore, the model can be said to give reasonable predictions for the incident peak overpressure.

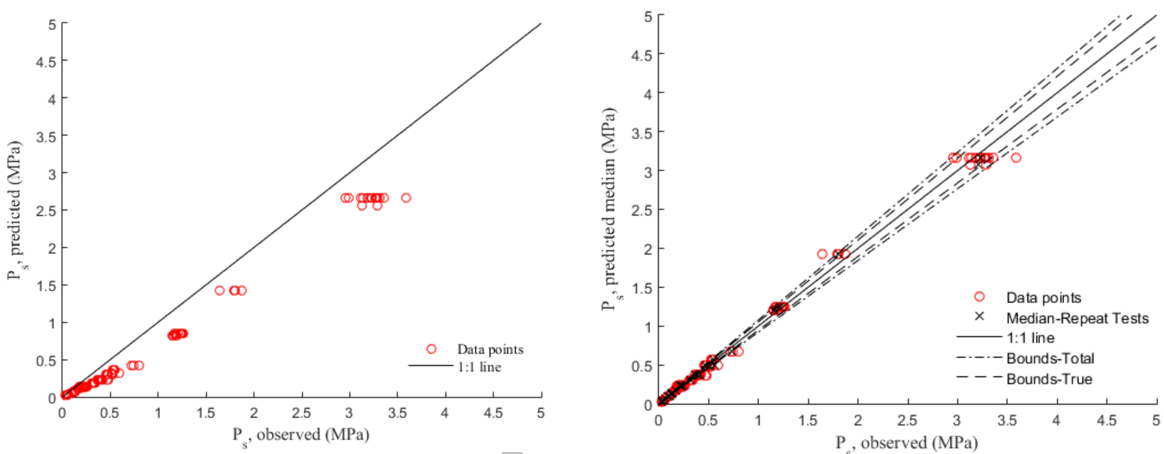


**Fig 3: Comparison between ratios of observed and measured incident peak overpressure based on deterministic (left) and probabilistic (right) models**

Fig. 4 shows the posterior COV of $\theta_{2,i}$'s (as dots) and mean of $\sigma_2$ (as an open square) at each step of the deletion process. The deletion process is stopped at the 13th step. Upon examining the correlation coefficients, we observe a high dependence between $\theta_{2,1}$ and $\theta_{2,4}$; and $\theta_{2,1}$ and $\theta_{2,8}$. Using Eq. (8), we combine them and the correction term for $P_r$, $\gamma_2$ is determined to be

$$\gamma_2\left(\mathbf{x},\boldsymbol{\Theta}_2\right)=\theta_{2,1}-\left(0.879+0.958\theta_{2,1}\right)\left[\ln\left(\frac{R}{r}\right)\right]+\left(2.5+1.056\theta_{2,1}\right)\left[\ln\left(\frac{R}{r}\right)\right]^2 \tag{20}$$

Please cite this document as: Singh, K., Gardoni, P., & Stochino, F. (2020). Probabilistic models for blast parameters and fragility estimates of steel columns subject to blast loads. *Engineering Structures*, *222*, 110944. DOI: 10.1016/j.engstruct.2020.110944

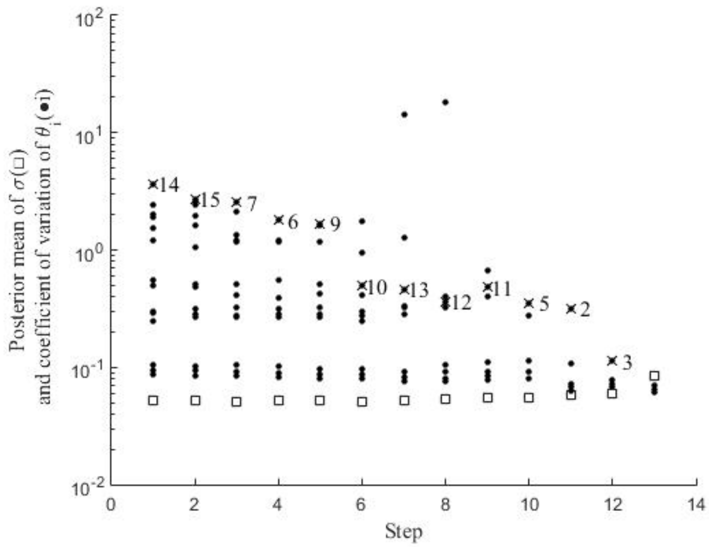


**Fig 4: Stepwise deletion for $\mathbf{\Theta}_2$, the cross points at the parameter with the higher coefficient of variation for each step.**

Table 3 lists the posterior statistics of $\mathbf{\Theta}_2$. The significant posterior statistics have the same behavior as those of $\mathbf{\Theta}_1$. Therefore, we can say that both deterministic models for peak overpressure underestimate the actual value and miss some information conveyed by $Z$.

**Table 3: Posterior statistics of $\mathbf{\Theta}_2$**

| Parameter | Mean | St. Dev. | Correlation Coefficients | |
|---|---|---|---|---|
| | | | $\theta_{2,1}$ | $\sigma_2$ |
| $\theta_{2,1}$ | –2.55 | 0.165 | 1 | |
| $\sigma_2$ | 0.075 | 0.005 | –0.016 | 1 |

Please cite this document as: Singh, K., Gardoni, P., & Stochino, F. (2020). Probabilistic models for blast parameters and fragility estimates of steel columns subject to blast loads. *Engineering Structures*, *222*, 110944. DOI: 10.1016/j.engstruct.2020.110944

Fig 5 shows a comparison between the ratio of the measured and predicted values of $P_r$ based on the deterministic (left) and probabilistic (right) models. The figure is developed like Fig 3. It can be observed that the correction terms effectively correct the bias in the deterministic model. For the probabilistic model, the median values of the ratios of observed and predicted values lie evenly between the one standard deviation limits, which includes the standard deviation of the measurement error.

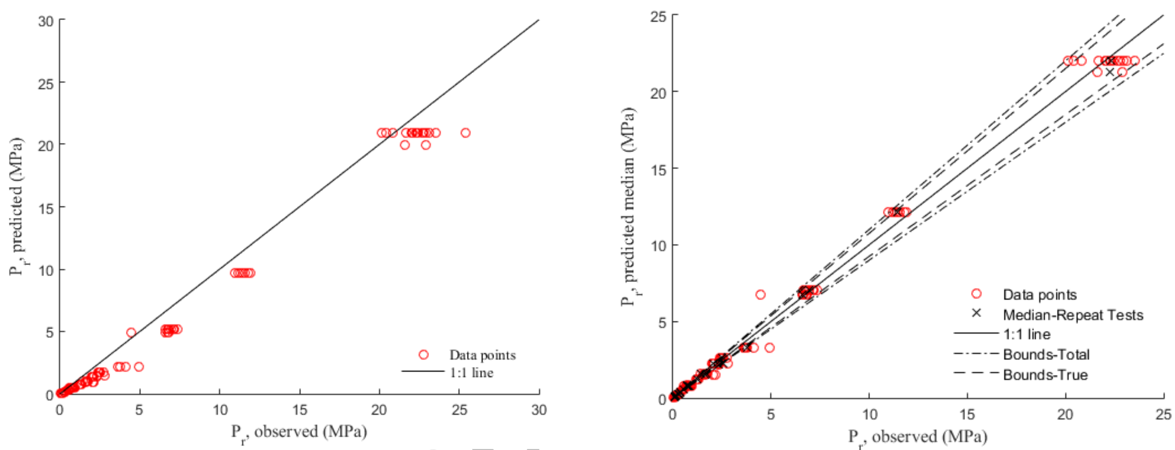


**Fig 5: Comparison between ratios of observed and measured reflected peak overpressure based on deterministic (left) and probabilistic (right) models**

Fig. 6 shows the posterior COV of $\theta_{3,i}$'s (as dots) and mean of $\sigma_3$ (as an open square) at each step of the deletion process. The deletion process is stopped at the 13$^{th}$ step. We observe strong correlation between $\theta_{3,4}$ and $\theta_{3,8}$. Using Eq. (8), we combine them and the correction term for $t_{d,i}$, we determine $\gamma_3$ to be

$$\gamma_3\left(\mathbf{x},\boldsymbol{\Theta}_3\right)=\theta_{3,4}\left[\ln\left(\frac{R}{r}\right)\right]+\theta_{3,5}\left[\ln\left(\frac{W}{\overline{\overline{W}}}\right)\right]+\left(0.42-1.015\theta_{3,4}\right)\left[\ln\left(\frac{R}{r}\right)\right]^2 \tag{21}$$

Please cite this document as: Singh, K., Gardoni, P., & Stochino, F. (2020). Probabilistic models for blast parameters and fragility estimates of steel columns subject to blast loads. *Engineering Structures*, *222*, 110944. DOI: 10.1016/j.engstruct.2020.110944

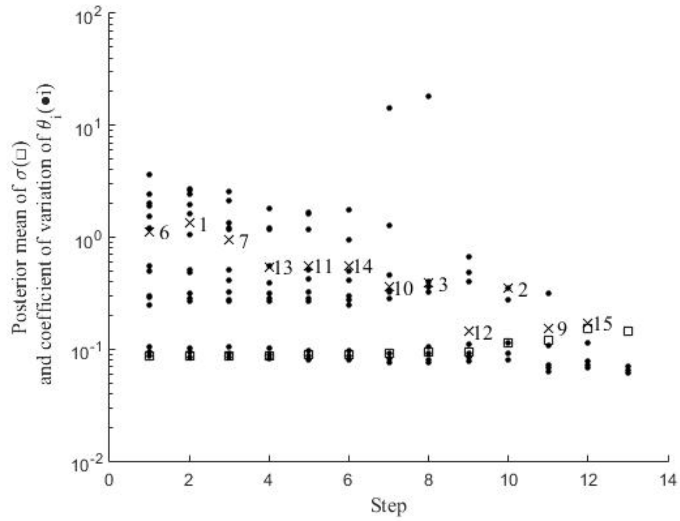


**Fig 6: Stepwise deletion for $\mathbf{\Theta}_3$, the cross points at the parameter with the higher coefficient of variation for each step.**

Table 4 lists the posterior statistics of $\mathbf{\Theta}_3$. On a closer examination of the parameters, we observe that there is no intercept term. Hence, there was no significant bias in the deterministic model. However, correction terms including the charge weight and the information from $Z$ are significant.

**Table 4: Posterior statistics of $\mathbf{\Theta}_3$**

| Parameter | Mean | St. Dev. | Correlation Coefficients | | |
|---|---|---|---|---|---|
| | | | $\theta_{3,4}$ | $\theta_{3,5}$ | $\sigma_3$ |
| $\theta_{3,4}$ | 0.207 | 0.024 | 1 | | |
| $\theta_{3,5}$ | −0.156 | 0.013 | −0.37 | 1 | |
| $\sigma_3$ | 0.145 | 0.008 | −0.06 | 0.004 | 1 |

Fig 7 shows a comparison between the ratios of measured and predicted values of $t_{d,i}$ based on the deterministic (left) and probabilistic (right) models. It can be observed that the correction terms decrease the spread of the observed values. For the probabilistic model, the ratios lie evenly between the one standard deviation limits of the true model error. The observation with the median ratio of 1.4 lies almost completely outside the bounds. However, the observations correspond to $Z = 0.58\ \text{kg/m}^{1/3}$. As per Kingery (1966), the observations of positive phase duration are difficult to measure and can be unreliable representations of the actual values for small scale distances. Therefore, more research needs to be done to ensure accurate recording of phase duration for small scale distances.

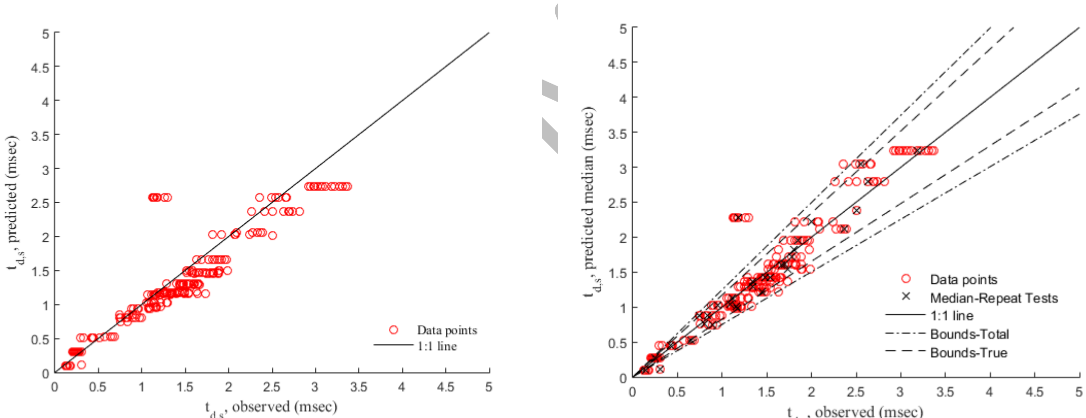


**Fig 7: Comparison between ratios of observed and measured incident positive phase duration based on deterministic (left) and probabilistic (right) models**

Fig. 8 shows the stepwise deletion process for the parameters of $\mathbf{\Theta}_4$. The deletion process is stopped at the 14th step. The intercept term $h_{4,1}$ and $h_{4,5}$ are determined to be the most significant functions in the correction term for $t_{d,r}$, i.e., $\gamma_4$ becomes:

Please cite this document as: Singh, K., Gardoni, P., & Stochino, F. (2020). Probabilistic models for blast parameters and fragility estimates of steel columns subject to blast loads. *Engineering Structures*, *222*, 110944. DOI: 10.1016/j.engstruct.2020.110944

$$\gamma_4\left(\mathbf{x},\mathbf{\Theta}_4\right)=\theta_{4,1}+\theta_{4,5}\left[\ln\left(\frac{W}{\bar{\bar{W}}}\right)\right] \tag{22}$$

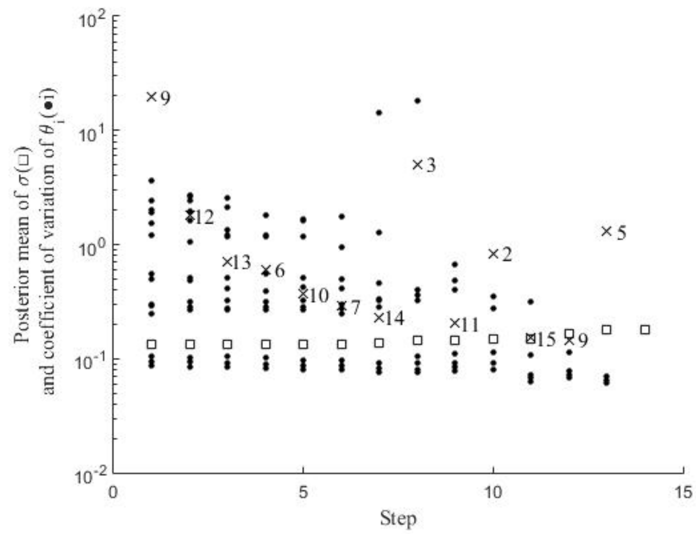


**Fig 8: Stepwise deletion for $\mathbf{\Theta}_4$, the cross points at the parameter with the higher coefficient of variation for each step.**

Table 5 lists the posterior statistics of $\mathbf{\Theta}_4$. The negative mean of intercept indicates that the deterministic model overestimates the reflected positive phase duration. Hence, there was significant bias in the deterministic model. However, the correction term including the charge weight is significant. Fig 9 shows a comparison between the ratios of measured and predicted values of $t_{d,r}$ based on the deterministic (left) and probabilistic (right) models. It can be observed that the correction terms decrease the spread of the observed values. For the probabilistic model, the ratios lie evenly between the one standard deviation limits, which includes the standard deviation of the measurement error.

**Table 5: Posterior statistics of $\mathbf{\Theta}_4$**

| Parameter | Mean | St. Dev. | Correlation Coefficients | | |
|---|---|---|---|---|---|
| | | | $\theta_{4,1}$ | $\theta_{4,5}$ | $\sigma_4$ |
| $\theta_{4,1}$ | –0.383 | 0.012 | 1 | | |
| $\theta_{4,5}$ | –0.178 | 0.012 | 0.28 | 1 | |
| $\sigma_4$ | 0.181 | 0.009 | –0.014 | 0.015 | 1 |

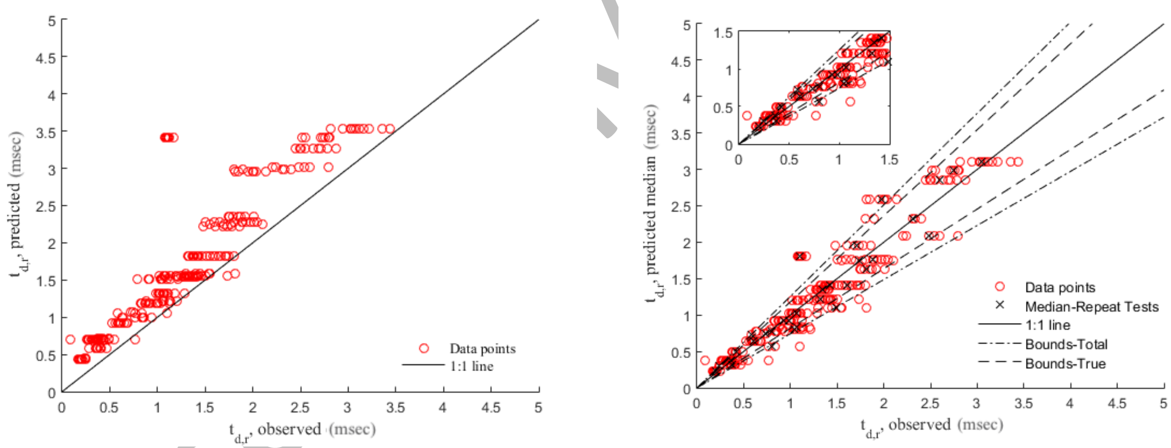


**Fig 9: Comparison between ratios of observed and measured reflected positive phase duration based on deterministic (left) and probabilistic (right) models**

## 4. Demand analysis of steel columns subject to blast loads

To determine the fragility curves for the mentioned limit states, we need to know the column probabilistic column demands for the limit states of flexure and global buckling. For the sake of simplicity, we will denote the column demand by $D_l(\mathbf{m}, \mathbf{\Theta}_o)$, where $l = 1, 2$ imply the limit states of flexure and global stability, respectively; $\mathbf{m}$ denotes the variables associated with the capacity and demand and; $\mathbf{\Theta}_o$ is the vector of the model parameters, where $o$ signifies the orientation of the column with respect to the blast load. We define $o = i$ for the incident case and $o = p$ for the perpendicular case. Therefore, $\mathbf{\Theta}_i = (\mathbf{\Theta}_1, \mathbf{\Theta}_3)$ and $\mathbf{\Theta}_r = (\mathbf{\Theta}_2, \mathbf{\Theta}_4)$. The matrix $\mathbf{m}$ can further be partitioned as $\mathbf{m} = (\mathbf{r}, \mathbf{s}_o)$, where $\mathbf{r}$ is a vector of material or geometrical properties, and $\mathbf{s}_o$ is a vector of demand variables such as boundary forces and deformations. For a steel column, Modulus of elasticity ($E_s$) and the yield strength ($y_s$) show significant variation which has to be incorporated within the probabilistic framework (Schmidt & Bartlett, 2002). Therefore, for our model, $\mathbf{r} = \{y_s, E_s\}$.

Actually, in next sections only the perpendicular reflected blast wave scenario is discussed and not the incident one. This is because the columns perpendicular to the blast wave in a building experience reflected blast waves due to the surrounding structure. Also, the reflected wave has higher impulse as $P_r$ is always higher than $P_s$ for same value of $Z$ (Karlos, 2013). Thus, the effect of reflected blast wave is critical for the fragility's assessment of a single column. However, the incident blast wave models can be useful in estimating the probability of progressive collapse when the roofs and the side walls will experience the impact of an incident blast wave.

Please cite this document as: Singh, K., Gardoni, P., & Stochino, F. (2020). Probabilistic models for blast parameters and fragility estimates of steel columns subject to blast loads. *Engineering Structures*, *222*, 110944. DOI: 10.1016/j.engstruct.2020.110944

*4.1. Single degree of freedom model for column analysis*

The single degree of freedom model assumes that a structural member can be represented by an equivalent spring-mass system, as shown in Fig 10. To calculate the response of the column, we solve the following equation of motion as given in Nassr et al., 2013:

$$K_M M\ddot{y} + K_L R(y) = K_L F(t) + K_L \eta(t) \tag{23}$$

or

$$K_{LM} M\ddot{y} + R(y) = F(t) + \eta(t) \tag{24}$$

where $\ddot{y}$ and $y$ correspond to the mid-span acceleration and displacement of the column; $M$ is the mass of the column; $F(t)$ is the lateral load imposed by the blast load; $R(y)$ is the resistance function; $\eta(t)$ is the equivalent lateral load due to the axial load $P$; $K_M$ and $K_L$ are the mass and load factors, and $K_{LM}$ is the load-mass transformation factor given by $K_{LM} = K_M / K_L$.

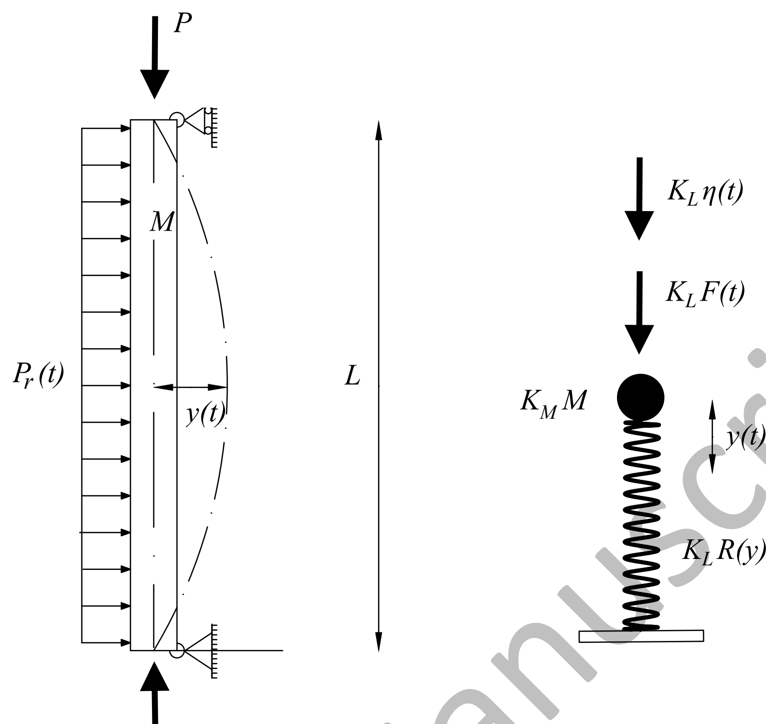


**Fig 10: Equivalent Single Degree of Freedom Model for Blast Loading**

The equivalent lateral load, represented by $\eta(t)$, is the secondary moment generated due to the eccentricity of the applied axial load and can be written as

$$\eta(t) = \frac{8P}{L} y(t) \tag{25}$$

The dynamic deformation can be approximated using the first vibration mode and shape function $\varphi$. The deformed shape varies with the support conditions and the deformation behavior of the member. For a simply supported beam, the shape functions chosen for the elastic and plastic ranges are

Please cite this document as: Singh, K., Gardoni, P., & Stochino, F. (2020). Probabilistic models for blast parameters and fragility estimates of steel columns subject to blast loads. *Engineering Structures*, *222*, 110944. DOI: 10.1016/j.engstruct.2020.110944

$$\phi(\xi)=\begin{cases}1-\dfrac{24}{5}\xi^2+\dfrac{16}{5}\xi^4 & \text{(elastic range)}\\ 1-|\xi| & \text{(plastic range)}\end{cases} \tag{26}$$

where $\xi = e/L - 1/2$ is a natural coordinate, $e$ is the cartesian axial coordinate of a point on the column measured from the left support and $L$ is the beam length. The values for the pinned-hinged end supports are taken from Biggs (1964) and are presented in table 6, where $K$ is the spring constant of the column and is equal to its elastic stiffness.

**Table 6: SDOF model parameter values for Pinned-hinged end supports**

| Deformation Regime | $K_L$ | $K_M$ | $K_{LM}$ | $R_y$ | Spring Constant $K$ |
|---|---|---|---|---|---|
| Elastic | 0.64 | 0.50 | 0.78 | $Ky(t)$ | $384\dfrac{EI}{L^3}$ |
| Plastic | 0.50 | 0.33 | 0.66 | $8\dfrac{M_p}{L}$ | 0 |

*4.2. Dynamic reactions and moments*

Once the displacement-time history is calculated using Eq. (24), we need to determine the dynamic reactions and mid-span moment. The dynamic reactions were calculated from the SDOF models using simplified expressions which were obtained based on the dynamic equilibrium of vertical forces (Biggs, 1964). Table 7 presents the expressions for dynamic reactions for a simply supported column. Nassr, 2012 validated that the expressions in Biggs (1964) provide a reasonably accurate approximation of the dynamic reactions for simply supported conditions despite neglecting the higher vibration modes.

**Table 7: Dynamic reactions for Pinned-hinged end supports**

| Deformation Regime | Dynamic Reactions |
|---|---|
| Elastic | $0.39R(t)+0.11F(t)$ |
| Plastic | $0.38R(t)+0.12F(t)$ |

Following Nassr (2012), we calculate the mid-span dynamic moments using the following expression based on dynamic equilibrium

$$M(t)=V_0\frac{L}{2}-P(t)w\frac{L^2}{2}-M\ddot{y}(t)\frac{1}{L}\int_0^{L/2}\phi(e)\left(\frac{L}{2}-e\right)de \tag{27}$$

where $w$ is the flange width, $V_0$ is the dynamic reaction and $P(t)$ is the blast overpressure.

The dynamic displacement and moments calculated will be used to check the column's adequacy against the blast loads, but it requires the knowledge of the column's capacity against moment and buckling. The next section gives a detailed explanation of the methods employed to calculate the column's moment and buckling capacity.

## 5. Capacity analysis of steel columns subject to blast loads

To determine the fragility curves for the mentioned limit states, we need to know the column capacities for the limit states of flexure and global buckling. Like the demand models, we denote the column capacity by $C_l(\mathbf{y}, \mathbf{\Theta}_k)$, where $l = 1, 2$ imply the limit states of flexure and global buckling.

### *5.1. Calculation of plastic moment capacity*

For the paper, we consider the steel column to achieve flexural failure when its moment capacity is achieved. To calculate the plastic moment capacity of the column, we use the methodology presented in Nassr et al. (2012). To consider the effect of varying strain rate over the depth of the column cross section, the cross section was divided in $n$ layers. The strain rate in the $i^{th}$ layer was determined using the following equation

$$F_i = \sigma_i \times DIF_i \times w_i \times \Delta s \tag{28}$$

where $\sigma_i$, $DIF_i$ and $w_i$ are the total stress, dynamic increase factor and width of the $i^{th}$ layer; and $\Delta s$ is the thickness of each layer. The dynamic increase factor considers the effect of strain rate on the yield stress and is calculated as

$$DIF_i = 1 + \left( \frac{\dot{\varepsilon}_i}{40} \right)^{0.2} \tag{29}$$

where $\dot{\varepsilon}_i$ is the strain rate in the $i^{th}$ layer. The strain rate is assumed to vary linearly over the cross-sectional depth and is calculated from the maximum strain-time history. The maximum strain at the column mid-span is measured as

$$\dot{\varepsilon}_{\max}\Big|_{z=\frac{L}{2}} = \phi''\Big|_{z=\frac{L}{2}} \frac{d}{2} y(t) = 4.8 \frac{d}{L^2} y(t) \tag{30}$$

The moment is then calculated as $M = \sum_{i=1}^{n} F_i y_i$, where $y_i$ is the distance of the $i^{th}$ layer from the neutral axis. This methodology is used to develop the moment-curvature diagram and consequently find the plastic moment capacity of the column.

*5.2. Analysis of global stability of the column*

A column subjected to axial loads can exhibit both flexural and axial buckling, i.e., the instability can be triggered by both blast and axial loads. The actual determination of global instability requires calculation of the derivatives and second derivatives of the deflection time history. This procedure can be computationally expensive in the framework of reliability analysis because of the large number of iterations involved. Therefore, we use the methodology presented in Dragos & Wu (2014) to determine the onset of global instability using a reduced resistance function which was defined as

$$R_r\left(y\right) = R\left(y\right) - \frac{8P}{L} y \tag{31}$$

Please cite this document as: Singh, K., Gardoni, P., & Stochino, F. (2020). Probabilistic models for blast parameters and fragility estimates of steel columns subject to blast loads. *Engineering Structures*, *222*, 110944. DOI: 10.1016/j.engstruct.2020.110944

where $y$ is the mid-span deflection. For a loading falling in the impulsive regime, i.e., with a small value of $t_{d,i}$, the deflection at which global instability occurs for an infinitely short duration blast load, $y_{g,i}$, was determined as

$$y_{g,i} = \frac{M_p}{P} \tag{32}$$

where $M_p$ is the plastic moment capacity of the column and is obtained as per Sec 5.1. For the quasi-static regime, i.e., a large value of $t_{d,i}$, the deflection at which instability occurs for a long duration blast load is determined by

$$y_{g,p} = \sqrt{\frac{y_{el} M_p}{P}} \tag{33}$$

where $y_{el}$ is the maximum elastic deflection of the column.

Eqs. (32) and (33) give the upper and lower bounds for the buckling capacity of the column. Thus, the actual value can lie anywhere between these two values, depending on the regime of the blast load. However, Dragos & Wu, (2014) observed small difference in the two values and therefore, we assume $y_{g,p}$ as the deflection capacity of the column. This will give us a reasonable estimate of the failure probability of a column by global buckling when subjected to a blast load, while keeping the calculations computationally efficient.

## 6. Fragility curves for steel columns subject to blast loads

The fragility of a structural component is defined as the conditional probability of attaining or exceeding prescribed limit states for a given set of boundary variables. The limit state function for the failure of the column in mode *k* can be depicted by the following mathematical model:

$$g_l\left(\mathbf{y},\mathbf{\Theta}_o\right)=C_l\left(\mathbf{y},\mathbf{\Theta}_o\right)-D_l\left(\mathbf{y},\mathbf{\Theta}_o\right) \qquad l=1,2 \tag{34}$$

In the equation, $g_l(\mathbf{y},\mathbf{\Theta}_o)\le 0$ denotes the failure of the structural component in the $l^{th}$ failure mode and $o$ denotes the orientation of the column with respect to the blast wave.

The failure fragility of the structural component can then be defined as:

$$F_l\left(\mathbf{s},\mathbf{\Theta}_o\right)=P\left[g_l\left(\mathbf{s},\mathbf{r},\mathbf{\Theta}_o\right)\le 0\,|\,\mathbf{s},\mathbf{\Theta}_o\right] \tag{35}$$

As the fragility is expressed as a function of the parameters $\mathbf{\Theta}_o$, the estimate is dependent on the treatment of the parameters. Gardoni et al. (2002) listed the various fragility estimates as

i. Point Estimates of Fragility
ii. Predictive Estimate of Fragility
iii. Bounds on Fragility

Point estimates predict the fragility based on the mean value of the parameters and therefore does not consider the variability in the model parameters $\mathbf{\Theta}_o$. Predictive estimates, on the other hand, incorporate the epistemic uncertainties in an average sense but do not give an idea about the variation of the fragilities w.r.t $\mathbf{\Theta}_o$. Traditionally, the exact evaluation of the distribution requires nested reliability calculations, but approximate confidence bounds can be obtained through FORM analysis as per the methodology given in Gardoni et al. (2002).

We determine the reliability index corresponding to the conditional fragility $F(\mathbf{s},\boldsymbol{\Theta}_o)$ as:

$$\beta\left(\mathbf{s},\boldsymbol{\Theta}_o\right)=\Phi^{-1}\left[1-F(\mathbf{s},\boldsymbol{\Theta}_o)\right] \tag{36}$$

Generally, $\beta(\mathbf{s},\boldsymbol{\Theta}_o)$ is less strongly nonlinear in $\boldsymbol{\Theta}_o$ than $F(\mathbf{s},\boldsymbol{\Theta}_o)$. Using a first-order Taylor series expansion around the mean point $M_{\boldsymbol{\Theta}_k}$, we can compute the variance of $\beta(\mathbf{s},\boldsymbol{\Theta}_o)$ as

$$\sigma_\beta^2(s)\approx\nabla_\Theta\beta(s)\Sigma_{\Theta\Theta}\nabla_\Theta\beta(s)^T \tag{37}$$

The 15% and 85% confidence bounds then correspond to $\beta_{predictive}\pm\sigma_\beta$ respectively.

6.1. Fragility curves for a steel column subject to blast loads

As an example, we use the developed models to estimate the fragility curves of a 3.5 m long $\mathrm{W6}\times16$ steel column subject to the blast load of a reflected blast wave generated from the explosion of 125 kg Pentolite. In this first analysis, the considered distance *R* is varying between 7.5 to 20 m (i.e., scaled distance between 1 and 4 m/kg$^{1/3}$) in order to ensure that the column experiences a uniform blast pressure. The yield strength and elastic modulus of steel are modeled as lognormal random variables, i.e., $y_s\sim LN(360.5,22.7)$ MPa and $E_s\sim LN(207.6,5.4)$ GPa. Figure 11 presents the fragility curves for limit states of flexure and global stability for an axial load of $0.15P_y$, where $P_y$ is the column's axial capacity.

Please cite this document as: Singh, K., Gardoni, P., & Stochino, F. (2020). Probabilistic models for blast parameters and fragility estimates of steel columns subject to blast loads. *Engineering Structures*, *222*, 110944. DOI: 10.1016/j.engstruct.2020.110944

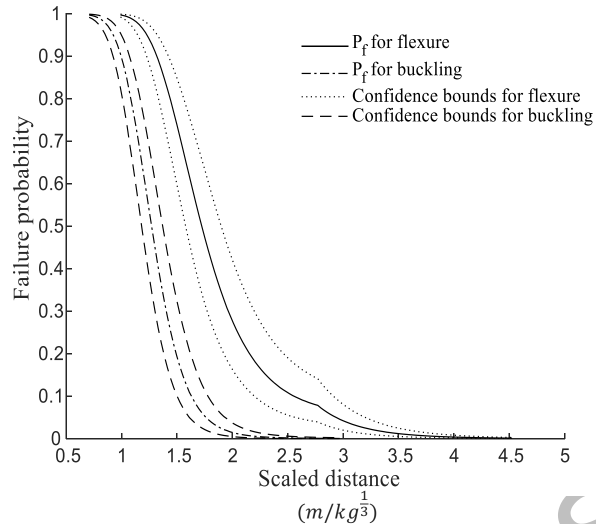


**Fig 11: Fragility curves for limit states of flexure and global buckling for $W6\times16$ with $P = 0.15P_y$**

We can observe that the flexure mode is always more likely than the global buckling mode. However, considering the global behavior of a framed structure a column flexural failure can be less dangerous than a column buckling failure which can be catastrophic and lead to progressive collapse. For this reason, both fragility curves are important. To further investigate the effect of charge weight on the fragility curves, Fig. 12 presents the comparison of flexural (left) and buckling (right) fragility curves for charge weights of 125 kg and 250 kg for $P = 0.15P_y$.

Please cite this document as: Singh, K., Gardoni, P., & Stochino, F. (2020). Probabilistic models for blast parameters and fragility estimates of steel columns subject to blast loads. *Engineering Structures*, *222*, 110944. DOI: 10.1016/j.engstruct.2020.110944

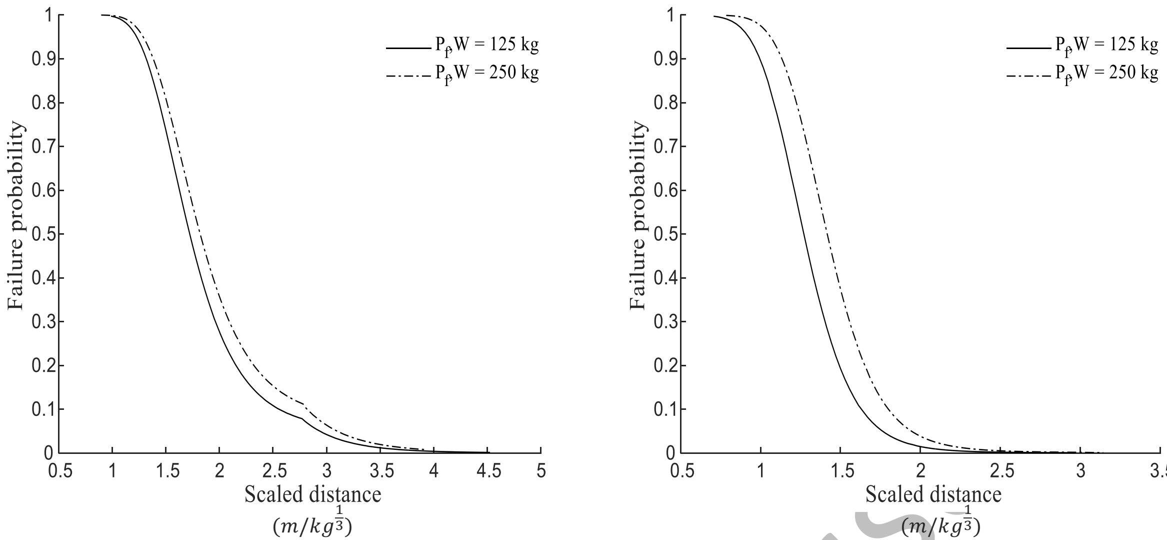


**Fig 12: Effect of charge mass on fragility curves for limit states of flexure (left) and global buckling (right)**

Since the fragility curves in Fig. 12 are very close, we do not include the confidence bounds. However, they are expected to follow the same behavior as the bounds in Fig. 11. As expected, the increase in charge mass increases the failure probabilities of the column at the same scaled distances. The increase can be attributed to two factors: the dependence of the deterministic models of positive phase duration on the charge weight; and the inclusion of charge weight in the correction term for reflective positive phase duration (Eq. 22).

The axial load on a column increases the demand and causes a decrease in the plastic moment capacity. Fig 13 shows the effect of increase in axial load on the flexural (left) and buckling (right) fragility curves.

Please cite this document as: Singh, K., Gardoni, P., & Stochino, F. (2020). Probabilistic models for blast parameters and fragility estimates of steel columns subject to blast loads. *Engineering Structures*, *222*, 110944. DOI: 10.1016/j.engstruct.2020.110944

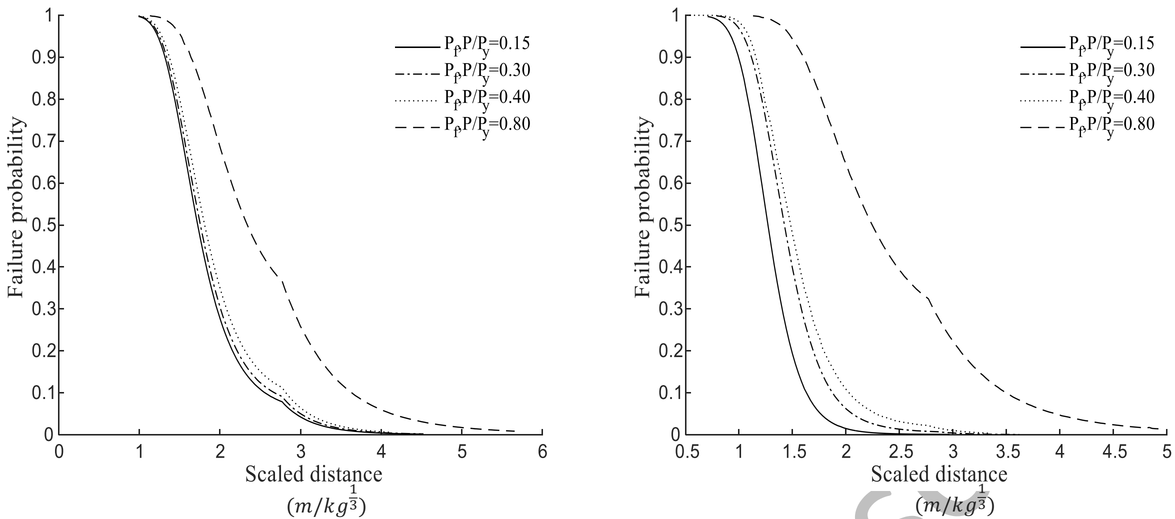


**Fig 13: Effect of axial load on fragility curves for limit states of flexure (left) and global buckling (right)**

Fig. 13 shows that the flexural fragility curves of the column do not experience any significant increase for columns loads between $0.15P_y - 0.40P_y$. The global buckling fragility curves experience a greater difference on the axial load, especially when the load was changed from $0.15P_y$ to $0.30P_y$. The results are significant from a design perspective as most columns have axial loads between $0.1P_y - 0.30P_y$. Thus, Fig. 13 implies that the buckling capacity of the column should be of concern for columns loaded above $0.15P_y$ to ensure sufficient collapse protection against blast loads. Fig.13 also shows that a column with an axial load close to the axial capacity is significantly vulnerable to blast loading.

In the fragility curves (Figures 11-13), there is a kink in the curves representing flexural collapse at $Z = 2.8$ m/kg$^{1/3}$. This can be attributed to the transition of deterministic equation for $t_{d,r}$ from Henrych (1979) to Kingery & Bulmash (1983). The slope of the fragility curves also changes as the rate of increase of $t_{d,r}$ decreases for $Z > 2.8$ m/kg$^{1/3}$.

## 7. Conclusions

Four probabilistic models are proposed to predict the parameters to determine the pressure-time behavior of blast waves. For different types of explosives and atmospheric conditions, two models predict the incident and reflected peak pressure generated by the explosion and two models predict the incident and reflected positive time duration of the blast wave. Simple correction terms are introduced in the probabilistic models to correct the inherent bias. The correction terms are developed by transforming initial candidate functions using the Box-Cox transformation. Higher order terms and interaction terms are included in the correction terms to account for the non-linear behavior of the parameters. The effect of measurement errors in the observed values and variability in the charge weight are also included. A stepwise deletion process is then used to develop parsimonious models, while maintaining an acceptable level of accuracy. The probabilistic models can be used to determine the variation in blast parameters for different types of explosives. Capacity and demand models for limit states of flexure and global buckling using the SDOF system are recognized from the literature and used to develop fragility curves for a steel column. The effects of charge weight and axial load on the fragility curves for the limit states are also presented. The results indicate that the plastic hinge mechanism occurs for much lower demands than required for the column failure. The results also indicate that the columns with high axial loads are more vulnerable to blast loads. The increase in charge mass also moderately increases the failure probabilities due to an increase in the positive phase duration.

Please cite this document as: Singh, K., Gardoni, P., & Stochino, F. (2020). Probabilistic models for blast parameters and fragility estimates of steel columns subject to blast loads. *Engineering Structures*, *222*, 110944. DOI: 10.1016/j.engstruct.2020.110944

**References**


Asprone, D., Jalayer, F., Prota, A., & Manfredi, G. (2010). Proposal of a probabilistic model for multi-hazard risk assessment of structures in seismic zones subjected to blast for the limit state of collapse. Structural Safety, 32(1), 25–34. https://doi.org/10.1016/j.strusafe.2009.04.002

Asprone D., Prota A., Manfredi G., (2008). Probabilistic assessment of blast-induced progressive collapse in a seismic retrofitted RC structure. 14thWCEE, October 12-17, 2008, Beijing, China.

Biggs, J. M. (1964). Introduction to structural dynamics. McGraw-Hill College, New York.

Box, G. E., & Cox, D. R. (1982). An analysis of transformations revisited, rebutted. Journal of the American Statistical Association, 77(377), 209–210. https://doi.org/10.1080/01621459.1982.10477788

Campidelli, M., Tait, M. J., El-Dakhakhni, W. W., & Mekky, W. (2015). Inference of Blast Wavefront Parameter Uncertainty for Probabilistic Risk Assessment. Journal of Structural Engineering, 141(12), 04015062. https://doi.org/10.1061/(asce)st.1943-541x.0001299

Denny, J. W., & Clubley, S. K. (2019). Long-duration blast loading & response of steel column sections at different angles of incidence. Engineering Structures, 178, 331-342.

Ding, Y., Song, X., & Zhu, H. T. (2017). Probabilistic progressive collapse analysis of steel frame structures against blast loads. Engineering Structures, 147, 679–691. https://doi.org/10.1016/j.engstruct.2017.05.063

Draganić, H., Gazić, G., & Varevac, D. (2019). Experimental investigation of design and retrofit methods for blast load mitigation–A state-of-the-art review. Engineering Structures, 190, 189-209.

Dragos, J., & Wu, C. (2014). Single-Degree-of-Freedom Approach to Incorporate Axial Load Effects on Pressure Impulse Curves for Steel Columns. Journal of Engineering Mechanics, 141(1), 04014098. https://doi.org/10.1061/(asce)em.1943-7889.0000818

Gardoni, P., Der Kiureghian, A., & Mosalam, K. M. (2002a). Probabilistic Capacity Models and Fragility Estimates for Reinforced Concrete Columns based on Experimental Observations. Journal of Engineering Mechanics, 128(10), 1024–1038. https://doi.org/10.1061/(ASCE)0733-9399(2002)128:10(1024)

Gardoni P, Mosalam KM, Der Kiureghian A. (2003) Probabilistic seismic demand models and fragility estimates for RC bridges. J Earthquake Eng; 7(spec01):79–106. https://doi.org/10.1142/S1363246903001024.

Haario, H., Laine, M., Mira, A., & Saksman, E. (2006). DRAM: Efficient adaptive MCMC. Statistics and Computing, 16(4), 339–354. https://doi.org/10.1007/s11222-006-9438-0

Hamburger, R., & Whittaker, A. (2004). Design of steel structures for blast-related progressive collapse resistance. Modern Steel Construction, 44(3), 45-51.

Hao, H., Hao, Y., Li, J., & Chen, W. (2016). Review of the current practices in blast-resistant analysis and design of concrete structures. Advances in Structural Engineering, 19, 1193–1223. https://doi.org/10.1177/1369433216656430

Heidarpour, A., & Bradford, M. A. (2011). Beam–column element for non-linear dynamic analysis of steel members subjected to blast loading. Engineering Structures, 33(4), 1259-1266.

Henrych, J. (1979). The dynamics of explosion and its use. Elsevier Scientific Publishing Company, Amsterdam & New York.

Hoffman, A.J. and Mills, S.N. (1956). Air Blast Measurements About Explosive Charges at Side-on and Normal Incidence. BRL Report No 988. US Army Armament Research and Development Centre, Ballistic Research Laboratory, Aberdeen Proving Ground, Maryland, USA.

Jia, G., Tabandeh, A., & Gardoni, P. (2017). Life-cycle analysis of engineering systems: Modeling deterioration, instantaneous reliability, and resilience. In Springer Series in Reliability Engineering. https://doi.org/10.1007/978-3-319-52425-2_20

Karlos, V., Solomos, G., & Larcher, M. (2017): Probabilistic analysis of steel columns under blast induced loads. Ce/Papers, 1(2–3), 3960–3969. https://doi.org/10.1002/cepa.452

Karlos, V., & Solomos, G. (2013). Calculation of blast loads for application to structural components. Report No JRC 32253-2011. Luxembourg: Publications Office of the European Union.

Khandelwal, K., El-Tawil, S., & Sadek, F. (2009). Progressive collapse analysis of seismically designed steel braced frames. Journal of Constructional Steel Research, 65(3), 699–708. https://doi.org/10.1016/j.jcsr.2008.02.007

Kingery C.N. (1966) Air blast parameters versus distance for hemisphericalTNT surface bursts. Ballistic Research Laboratories Report No. 1344,September 1966.

Kingery, Charles N., & Coulter, G. A. (1983). Reflected Overpressure Impulse on a Finite Structure. Retrieved from http://www.dtic.mil/dtic/tr/fulltext/u2/a137259.pdf

Kingery C. N., & Bulmash G., (1984) "Technical report ARBRL-TR-02555: Air blast parameters from TNT spherical air burst and hemispherical burst", AD-B082 713, U.S. Army Ballistic Research Laboratory, Aberdeen Proving Ground, MD.

Kinney Gilbert, Graham Kenneth. Explosive shocks in air. Berlin and New York: Springer-Verlag; 1985.

Krauthammer, T., Shahriar, S., & Shanaa, H. M. (1990). Response of reinforced concrete elements to severe impulsive loads. Journal of Structural Engineering, 116(4), 1061-1079. https://doi.org/10.1061/(ASCE)0733-9445(1990)116:4(1061)

Krauthammer, T. (2003). AISC research on structural steel to resist blast and progressive collapse, in Proceedings of AISC Steel Building Symposium: Blast and Progressive Collapse Resistance, pp. 67–81, New York, NY, December 2003, USA.

Lee, K., Kim, T., & Kim, J. (2009). Local response of W-shaped steel columns under blast loading. Structural Engineering and Mechanics, 31(1), 25–38. https://doi.org/10.12989/sem.2009.31.1.025

McConnell, J. R., & Brown, H. (2011). Evaluation of progressive collapse alternate load path analyses in designing for blast resistance of steel columns. Engineering Structures, 33(10), 2899-2909.

Nassr, A. A., Razaqpur, A. G., Tait, M. J., Campidelli, M., & Foo, S. (2012). Single and multi degree of freedom analysis of steel beams under blast loading. Nuclear Engineering and Design, 242, 63–77. https://doi.org/10.1016/j.nucengdes.2011.10.020

Nassr, A. A., Razaqpur, A. G., Tait, M. J., Campidelli, M., & Foo, S. (2013). Strength and stability of steel beam columns under blast load. International Journal of Impact Engineering, 55, 34–48. https://doi.org/10.1016/j.ijimpeng.2012.11.010

Nassr, A. a. (2012). Experimental and Analytical Study of the Dynamic Response of Steel Beams and Columns To Blast, Doctoral Dissertation, McMaster University, Hamilton, Ontario, Canada.

Netherton, M. D., & Stewart, M. G. (2010). Blast Load Variability and Accuracy of Blast Load Prediction Models. International Journal of Protective Structures, 1(4), 543–570. https://doi.org/10.1260/2041-4196.1.4.543

Netherton, Michael D. (2012). Probabilistic Modelling of Structural and Safety Hazard Risks for Monolithic Glazing Subject to Explosive Blast Loads. Doctoral dissertation, Ph. D. thesis, Univ. of Newcastle, Newcastle, Australia.

Ngo, T., Mendis, P., Gupta, A., & Ramsay, J. (2007). Blast loading and blast effects on structures - An overview. Electronic Journal of Structural Engineering, 7, 76–91.

Olsson, U. (2005). Confidence intervals for the mean of a log-normal distribution. Journal of Statistics Education, 13(1). https://doi.org/10.1080/10691898.2005.11910638

Sabuwala, T., Linzell, D., & Krauthammer, T. (2005). Finite element analysis of steel beam to column connections subjected to blast loads. International Journal of Impact Engineering, 31(7), 861–876. https://doi.org/10.1016/j.ijimpeng.2004.04.013

Schmidt, B. J., & Bartlett, F. M. (2002). Review of resistance factor for steel: resistance distributions and resistance factor calibration. Canadian Journal of Civil Engineering, 29(1), 109–118. https://doi.org/10.1139/L01-082

Shi, Y., Hao, H., & Li, Z. X. (2008). Numerical derivation of pressure-impulse diagrams for prediction of RC column damage to blast loads. International Journal of Impact Engineering, 35(11), 1213–1227. https://doi.org/10.1016/j.ijimpeng.2007.09.001

Tabandeh, A., & Gardoni, P. (2014). Probabilistic capacity models and fragility estimates for RC columns retrofitted with FRP composites. Engineering Structures, 74, 13–22. https://doi.org/10.1016/j.engstruct.2014.05.005

UFC 3-340-02. (2008). UFC 3-340-02 Structures to Resist the Effects of Accidental Explosions. In Structures Congress 2011. https://doi.org/10.1061/41171(401)127

Urgessa, G. S., & Arciszewski, T. (2011). Blast response comparison of multiple steel frame connections. Finite Elements in Analysis and Design, Vol. 47, pp. 668–675. https://doi.org/10.1016/j.finel.2011.01.009

Weisberg, S. (2005). Applied Linear Regression, John Wiley & Sons, NY, US.

Zhang, C., Gholipour, G., & Mousavi, A. A. (2019). Nonlinear dynamic behavior of simply-supported RC beams subjected to combined impact-blast loading. Engineering Structures, 181, 124-142.